

Thermal Shock and Oxidation Stability Tests to Grade Plasma Sprayed Functionally Gradient Thermal Barrier Coatings

Pasupuleti Kirti Teja ^a, Parvati Ramaswamy ^{a,*}, S.V.S. Narayana Murthy ^b

^a, Department of Mechanical & Automobile Engineering, Faculty of Engineering, CHRIST (Deemed to be University) Bangalore, India.

^b Materials Characterization Division, Vikram Sarabhai Space Center, Trivandrum, India.

***Corresponding Author**

parvati.ramaswamy@christuniversity.in

(Parvati Ramaswamy)

Received : 6th January 2019

Accepted : 28th February 2019

ABSTRACT: Functionally graded layers in thermal barrier coatings reduce the stress gradient between the overlaid ceramic coatings and the underlying metallic component. Introduced to alleviate early onset of spallation of the coating due to thermal expansion mismatch, this facilitates improvement in the life of the component. Conventional thermal barrier coatings typically comprise of duplex layers of plasma sprayed 8% yttria stabilized zirconia (ceramic) coatings on bond coated (NiCrAlY) components/substrates (Inconel 718 for example). This work highlights the superiority of plasma sprayed coatings synthesized from blends of the intermetallic bond coat and ceramic plasma spray powders on Inconel 718 substrates in three-layer configuration over the duplex layered configuration. Assessed through (a) thermal shock cyclic tests (at 1200°C and 1400°C) in laboratory scale basic burner rig test facility and (b) oxidation stability test in high temperature furnace (at 800°C and 1000°C) the functionally graded coatings of certain configurations exhibited more than double the life of the conventional 8% yttria stabilized zirconia duplex (double layer) coatings. Micro- and crystal structure analysis support the findings and results are detailed and discussed.

Keywords: Thermal Barrier Coatings, Functionally Gradient Materials, Plasma Spray

1. Introduction

1.1 Thermal Barrier Coatings

Thermal Barrier Coatings (TBCs) are ceramic materials, applied on metals to make their surfaces thermally insulating and to protect them from thermal degradation. Applied in the form of either thin (200–500µm) or thick (> 1 mm) coatings, industrial applications of TBCs are vast and varied such as in gas turbine, diesel, and aircraft engines [1,2]. TBCs in general, protect aerospace components from degradation at their high service temperature (>1000°C) environment, extend life and which in turn increase the performance efficiency of the aircraft engines. Typically, TBCs thicknesses are in the range of 120µm - 250µm which are comprised of low thermal conductivity material layer with suitable adhesion characteristics and microstructures [3,4]. Conventional TBC is applied to achieve adhesion of ceramic top coat over the metal component's surface through double layered coatings, namely, bond coat and ceramic top coat. The bond coat is an inter-metallic coating, 50 µm – 120 µm thick, applied above the pre-prepared metallic component surface, which develops an adhesive layer over the surface for the ceramic coating to bond. It also provides relief from the damage caused by the thermal

expansion mismatch between the metal substrate and ceramic over layer [5].

Atmospheric Plasma spraying (APS) is a well-established method to fabricate TBCs with yttria (usually 8% Y₂O₃) stabilized zirconia (ZrO₂) and NiCrAlY bond coat (BC) configuration. Popularly known as 8YSZ TBCs, they possess low thermal conductivity, suitable microstructure, thermal fatigue characteristics, mechanical properties and provide protection from damage due to oxidation at high service temperature [6,7]. TBCs protect the metal substrate and parts from thermal degradation (oxidation) and therefore increase their thermal fatigue life. However, large differences in the thermal expansion characteristics of the ceramic materials and underlying base metal results in poor adhesion between the metal ceramic interface especially in service at high operating temperatures [8]. In addition to oxidation, stress buildup between the ceramic coated layers and at the interface contribute further to the adhesive failure and sometimes within inter-ceramic layers known as cohesive failure.

8YSZ is the currently the most popular TBC system. The Stabilization of the m-ZrO₂ (unstabilized monoclinic zirconia) with a dopant is carried out to stabilize the stable t-

ZrO₂ (stabilized tetragonal zirconia) at room temperature. This is because unstabilized m-ZrO₂ transforms into tetragonal ZrO₂ at temperatures above 1000°C and this is a temperature related reversible transformation. The transformation is accompanied by a reversible volume change of about 3–5%, when cycled between room temperature and at temperatures above 1000°C, resulting in their spallation. Therefore, the transformation is suppressed and the high temperature tetragonal/cubic (t/c) ZrO₂ phase is stabilized at room temperature, which eliminates the spallation due to thermal expansion issues. While the thermal conductivity of 8YSZ is suitable for gas turbine TBCs applications, this material also suffers by being prone to sintering above 1200°C, resulting in an increase of the thermal conductivity at those temperatures making the TBC less effective. Furthermore, there is reduction in tolerance to thermal stresses and the associated strains due to the sintered and densified coatings. These effects can reduce the TBCs durability to a large extent and raise adhesion issues at and above 1200°C [9,10].

The problem described above can be overcome to an appreciable extent by processing the TBCs in suitably tailored different layers, encompassed of material (ceramic and bond coat i.e. 8YSZ and NiCrAlY respectively) layers with gradually varying thermal expansion characteristics. This is done via combination of two or more different types of coating materials, with optimized coating characteristics [11,12]. The formation of layers with different thermal expansion characteristics are achieved by providing intermediate layers sandwiched between the base bond coat (BC) and the final top coat (TC). They are comprised of blends of the BC and TC. Thus, with this new concept of composite having gradual compositional and/or microstructural variation over definable geometric orientations and by distances, three or multilayered functionally graded materials (FGM) are obtained which significantly improve the double layered 8YSZ TBCs characteristics [13,14].

The usage of FGM configurations is expected to reduce delamination remarkably within the inner layers. Even in the FGM system the ceramic layer, being the outermost layer is exposed to the harsh environment (at high temperatures) and provides the maximum protection. However, the ceramic does not end abruptly: rather being blended with bond coat, the layers below the ceramic experience gradual compositional change from being rich in ceramic to being rich in metal as moving towards the component interior [15,16]. Thus, in FGM systems, there is a strong potential for decreasing damage due to mis-match in properties amongst the TBC and the substrate. This is because the interfacial layers allow smooth transition of properties and possess higher fracture toughness. Hence a TBC built in FGM configuration is expected to be more resistant to delamination and exhibit higher durability characteristics compared to conventional TBC. Depending upon application,

the gradient (or the graded) layer can be classified on basis of different parameters. They may be (a) microstructural (b) multilayers of metals, ceramics or (c) comprised of layers integrated with different densities/porosities etc., [17]. In conventional TBC system, initially the bond coat (NiCrAlY) is coated to the desired thickness on the prepared metal substrate and next, layers of the ceramic coats (say 8YSZ) are applied on the top up to the desired or the most technically feasible thicknesses.

1.2 Functionally Graded Materials

Functionally Graded Materials (FGMs) can be synthesized in different ways. The most accepted method uses pre-alloyed feedstock powders to plasma spray the desired compositions [16]. The feed stock powders are generally synthesized by weighing the desired proportions of the bond coat and ceramic top coat (e.g. 25-75 or 50-50 ceramic-bond coat blend ratio etc.), blending, ball milling the blended powders followed by plasma spheroidization by plasma spraying into water by using the plasma torch. These powders are used as the feed stock for plasma spray coating. Using pre-alloyed feed stock powders offers several advantages: high deposition, more uniform coating density and improvement in chemical homogeneity [16].

Another method also involves blending of the constituent powders such as the bond coat and ceramic top coat in desired proportions [18]. However, the blends are directly plasma sprayed to form the coatings/FGM intermediate layers. This method although simpler, is likely to be associated with in-homogenous composition to some extent, within the same layer at different locations. A small variation to this process involves utilizing more than one torch at the same instance of spray coating, but the challenge lies in dictating the spray parameters to obtain uniform and consistent coated layers. The challenges in both these methods may be ascribed to the difference in densities, sizes, melting points and flowability possessed by the two kinds of spray powders [19]. While the superiority of pre-alloyed feed stock powders is unchallengeable, the process is relatively more expensive and technology driven than the simpler blended mixtures used as plasma spray powder. The effects of interaction between the particles and homogenization of particulate FGM in blend configuration, where the participating materials have significant variation in properties, cannot be overlooked. Nevertheless, this method is sufficient and useful to make preliminary assessment of the advantages of any one or more blended pattern over the base material. Upon establishing the most suited blend configuration, that particular FGM may be synthesized by pre-alloying the feedstock powder prior to plasma spraying [16, 20]. It is well known that FGM needs collaboration, involving more industries and international alliance to achieve the desired milestones to develop an industrial product, although small advancements in

understanding the concepts may be highly beneficial to the research community.

In addition to producing the FGMs, there is a strong need in terms of quality, reproducibility, reliability. The test methods involve the physical, chemical and mechanical behaviour of the FGMs and their correlation to the microstructure and their formation mechanism to control the fabrication process. Thus characterization plays an important role in the FGM development which should also match with the application envisaged.

Keeping this information in view, the current work focuses on the formation of FGMs by using the NiCrAlY inter-metallic bond coat and 8YSZ ceramic top coat plasma sprayable powders in different combinations of proportions, in form of blends prior to plasma spray coating on aerospace alloy substrates. Considering the FGMs are Thermal Barrier Coatings, thermal tests were performed to evaluate their characteristics. Comparisons were drawn with the duplex 8YSZ conventional TBCs as the baseline material.

2. Experimental procedure

2.1. Plasma Sprayed Coatings

Nickel based aerospace related super alloy (Inconel 718) base plates were used as substrates to synthesize the various configurations of FGMs in this work. AMDRY 962 (NiCrAlY) and METCO 204NS (8% YSZ) plasma sprayable powders were used as the bond coat (BC) and top coat (TC) respectively.

The two types of substrate plates used were (a) 50 mm X 10 mm X 5 mm: for oxidation stability test and (b) 80 mm X 75 mm X 5 mm: for thermal shock tests.

The substrates were blasted with alumina grits, degreased with a solvent following which bond coat was deposited on the surface over prior to the plasma spray coating of the FGM layers. The coatings were synthesized by using robot controlled Atmospheric Plasma Spray (APS 100 KW Metco Sulzer) facility. Table 1 shows APS parameters for

the bond coat and ceramic powder. All blends were spray coated by using spray parameters for the ceramic.

Table 1. APS parameters.

Parameter	NiCrAlY (BC)	8YSZ (TC)
Primary gas, Ar (l/min)	57	38
Power feed rate (gm/min)	45	35
Secondary gas, H ₂ (l/min)	14	17
Voltage (V)	75	70
Current (A)	400	550
Spray distance (mm)	10	10

2.2 Coatings Configuration

The design configuration of the coatings that were prepared is listed in Table 2

All the coated layers were plasma sprayed onto the prepared substrates. The details of the design configuration (reflected in Table 2) are described as the following

(a) Conventional:

- (i) First coated layer on grit blasted surface: Bond coat (BC) : 75 μm thick
- (ii) Second coated layer on bond coated surface: Top coat (TC): ~250 μm thick (Final layer)

(b) Functionally Graded Materials (FGM) Configuration:

(1) FGM 1 configuration:

- (i). First coated layer on grit blasted surface: BC: 75 μm thick
- (ii). Second coated layer) on bond coated surface: blend of 25BC+75TC: ~100 μm thick (intermediate layer)
- (iii). Third coated layer over intermediate layer surface: TC ~ 150 μm thick (Final layer)

Table 2. Coating Configuration (blend percentage & coating thickness)

Designation	Blend Configuration (weight %) (BC+ TC)	Thickness (μm) (BC)	Thickness (μm) Blend	Thickness (μm) (TC)
Conventional TBC	Nil	75 μm	Nil	250 μm
FGM 1	25BC + 75TC	75 μm	100 μm	150 μm
FGM 2	50BC + 50TC	75 μm	100μm	150 μm
FGM 3	60BC + 40 TC	75 μm	100 μm	150 μm

FGM 2 configuration:

- (i) First coated layer on grit blasted surface: BC: 75 μm thick
- (ii) Second coated layer on bond coated surface: blend of 50BC+50TC: $\sim 100 \mu\text{m}$ thick (intermediate layer)
- (iii) Third coated layer over intermediate layer surface: TC $\sim 150 \mu\text{m}$ thick (Final layer)

(3) FGM 3 configuration:

- (i) First coated layer on grit blasted surface: BC: 75 μm thick
- (ii) Second coated layer on bond coated surface: blend of 60BC+40TC: $\sim 100 \mu\text{m}$ thick (intermediate layer)
- (iii) Third coated layer over intermediate layer surface: TC $\sim 150 \mu\text{m}$ thick (Final layer)

The blends were prepared according to design ratio shown in Table 2 by weighing the bond coat (NiCrAlY) and the top coat (8YSZ) plasma sprayable powders separately. While mechanical mixing may not be the best method to synthesize a homogenous blend, this method was considered suitable to make a preliminary assessment of the concept of FGM. The identified powders and the composition of the two powders to form the blend were mixed manually for an hour right before the spray process. This was done to minimize the negative effects of segregation due to variable densities of the constituents. The intermediate blend powders thus prepared were then plasma spray coated on the bond coated surfaces by using a single plasma torch. Details of tests performed on the spray coated substrates are given below

2.3 Thermal shock (fatigue) Test.

Thermal shock cycling test emphasizes on ceramic coating surface being subjected to heat at high and low temperatures (interchanged) to observe the changes in the coating characteristics and degradation/failure occurrences caused by stresses especially due to thermal expansion. Generally some variations in the test methods have been practiced by various researchers [21]. The main methodology of test however, is generally based on standard and established ASTM tests, e.g. ASTM D 6944 - 15 [22].

Thermal cycling forms one of the few highly important deciding factors to determine the life time for the TBCs under service conditions involving high temperatures. In the present work, the outermost layer (ceramic) surface was exposed to a source of heat suddenly, to reach a prefixed high temperature (1200°C and 1400°C in this case), held at that temperature for a prefixed time before removing the heat source: followed by exposure to a cooling medium for a prefixed time. The heating source was an oxy-acetylene flame, the source to cool the hot ceramic surface was 'forced air' in ambient room temperature ($\sim 25^\circ\text{C}$) and the holding times at the time of rapid heating and rapid cooling were 60

seconds each time. This entire process of rapid heating, holding and rapid cooling comprised of one test cycle. The ceramic coating surface temperature was measured using a non-contact infra-red thermometer gun.

Severe thermal stresses are expected to be induced in the coating during the thermal shock cycling test process. Stresses are expected to be produced due to the mismatch in the thermal expansion characteristics between the top coat, and the metallic bond coat. The capability of the intermediate layers in alleviating the stresses and to prolong the life of the TBC system was being explored in this work.

2.4 Oxidation Stability Test

Oxidation stability characteristics help to understand the influence of oxidation on the underlying metal below the TBCs. In addition to the increased oxygen ionic conductivity at high temperatures ($>800^\circ\text{C}$), porosities in the coatings play an important role in oxygen transport through them and thereby significantly influence the metal substrate degradation. Therefore, in order to extend the life of the component on which TBC is applied, not only should there be good adherence between the bond coat and top coat but also must be synthesized with optimum porosity for best (low) thermal conductivity and minimum oxygen transport characteristics. In service, due to prolonged heating there is a progressive change in area of contact between the bond coat and top coat due to the formation of thermally grown oxide (TGO) [23,24]. Increased oxidation transport is not desirable in these systems and it is important to control the growth of TGO. Reportedly [25, 26] TGO, when allowed to grow beyond a threshold value of 6-7 μm , exerts severe compressive stresses on the overlaid coatings, resulting in tensile stresses in the ceramic layers of which therefore are unable to remain intact and flake off. The study of the influence of the FGM microstructure in controlling the porosity in the microstructure and the oxidation characteristics as well was attempted in this work.

To carry out the oxidation stability test, Inconel718 test bars of dimension 50 mm X 10 mm X 5 mm were coated on all sides as per the design configuration (Table 2) and tested at 800°C and 1000°C by employing a muffle furnace. The coated test bars were introduced into the high temperature furnace at ambient temperature and gradually rising the temperature of the furnace to the required temperature and holding for 12 hours followed by furnace cooling to normal ambient temperature inside the furnace. The specimens was removed and examined with naked eyes or under low power magnification (10X) for any defects. If the coatings were damaged (cracked, peeled off or degraded) the test was stopped. If not, the cycle was repeated until the coating on the specimen showed signs of damage.

2.5 Characterization

2.5.1 Microstructure and Structural phase analysis

Scanning Electron Microscope (SEM) was employed to analyze the metallographic polished cross sections removed from the as-sprayed specimen and those subjected to thermal tests. The substrate-coating interface and its microstructure were examined in detail. X-ray diffractometer (XRD) was used to carry out the structural phase analysis of the coated specimens.

3. Results

3.1 Microstructure of As-sprayed Coatings

Fig 1 shows the microstructures of as sprayed coatings of (a) Conventional 8YSZ (b) FGM 2 (typical) TBCs when studied in polished cross section metallographic specimen.

(a) Conventional Coating: ~ 65 μm thick bond coat ~310 μm thick top coat (YSZ) was measured from the SEM micrograph (Fig 1a).

3.2 Thermal shock (fatigue) test performances of Conventional and FGM TBCs

In this test, the thermal fatigue characteristics of the sample and the number of thermal cycles (heating and cooling cycles) through which the sample have gone through has been highlighted in Table 3 and Table 4 shows the summarized results of thermal shock test at 1200°C and 1400 °C.

From these results it is observed that an introduction of FGM layer between the bond coat and ceramic coat layers in TBC shows high potential in extending the life of duplex coatings under the thermal shock cycles test conditions adopted in this work. The other parameters such as thermal conductivity, mechanical stresses associated with the introduction of an intermediate third layer warrants detailed investigation though.

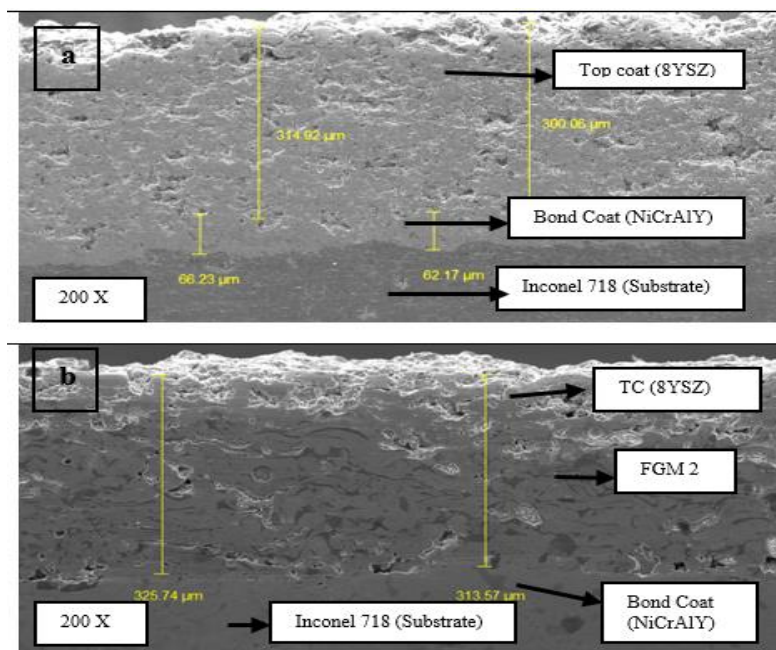


Fig 1. SEM image of As-sprayed cross-sectioned specimen: a) Conventional TBC; b) FGM 2 TBC

Table 3. Results of Thermal Shock Test at 1200°C

S.No	Specimen Designation	Bond Coat BC(μm)	Blended Configuration Wt %(BC+(C)) (μm)	Top coat (C) (μm)	Number of cycles	Remarks
1	Conv TBC	75	---	300	156	Failed
2	FGM 1	75	150	150	162	Failed
3	FGM 2	75	150	150	182	Not Failed (Test Stopped)
4	FGM 3	75	150	150	170	Not Failed (Test Stopped)

Table 4. Results of Thermal Shock Test at 1400°C

S.No	Specimen Designation	Bond Coat BC (µm)	Blended Configuration Wt %(BC+ TC) (µm)	Top coat (C) (µm)	Number of cycles	Remarks
1	Conv. TBC	75	---	300	182	Failed
2	FGM 1	75	150	150	174	Failed
3	FGM 2	75	150	150	210	Not Failed (Test Stopped)
4	FGM 3	75	150	150	184	Not Failed (Test Stopped)

Table 5. Findings from the XRD patterns

Sl No.	Reference in Fig 2	Sample Details Thermal shock cycling @ 1200°C (XRD on outer most surface)	Findings from XRD pattern	Remarks
1.	a	Conventional as-sprayed	(%) c/t-ZrO ₂ = 100	No destabilization
2.	b	Conventional – Failed (156 cycles)	(%) c/t-ZrO ₂ = 100	No destabilization
3.	c	FGM 1 – Failed (162 cycles)	(%) c/t-ZrO ₂ = 98 (%) m -ZrO ₂ = 2	Mild destabilization
4.	d	FGM 2- Not Failed (182 cycles)	(%) c/t-ZrO ₂ = 84 (%) m -ZrO ₂ = 16	Significant destabilization
5.	e	FGM 3- Not Failed (170 cycles)	(%) c/t-ZrO ₂ = 94 (%) m -ZrO ₂ = 6	Moderate destabilization

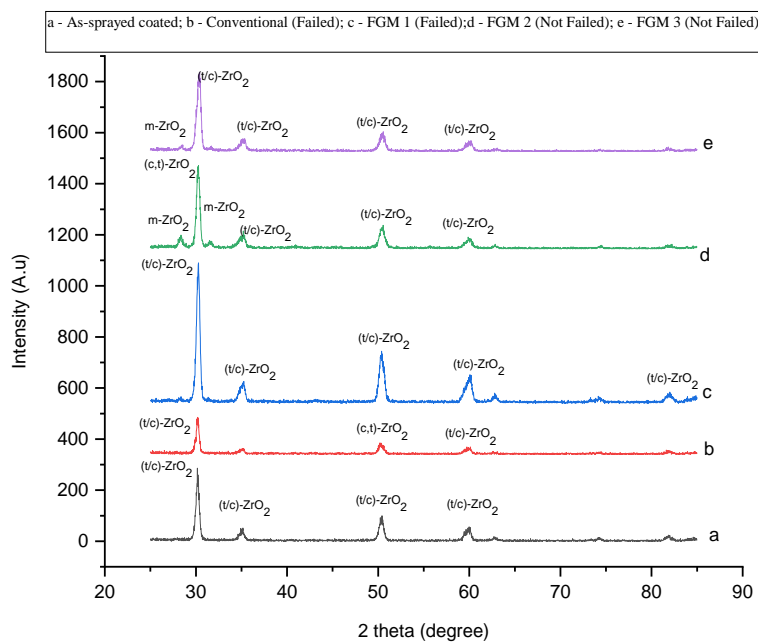


Fig 2. XRD patterns of thermal shock specimen of conventional and various FGM configurations at 1200°C

3.3 X-Ray Diffraction Analysis on thermal Shock tested specimen **3.4 Oxidation stability Test**

The XRD patterns of as-sprayed coated and thermal shock test specimen of conventional and various FGM configurations at 1200°C is shown in the Fig 2. Table 5 shows the findings from the XRD patterns shown in the Fig 2. Table 5 shows the findings from the XRD patterns shown in the Fig 2

The results obtained after conducting oxidation stability test on conventional and FGM blended configuration, at 800°C are shown in Fig 3: shows (a) the conventional TBCs samples failed in 96 hours of test and (b) blended configuration (FGM 1, FGM 2 and FGM 3) not failed even after 264 hours of testing. Similarly, the specimen also underwent oxidation stability test at 1000°C. Results are shown in Fig 4.

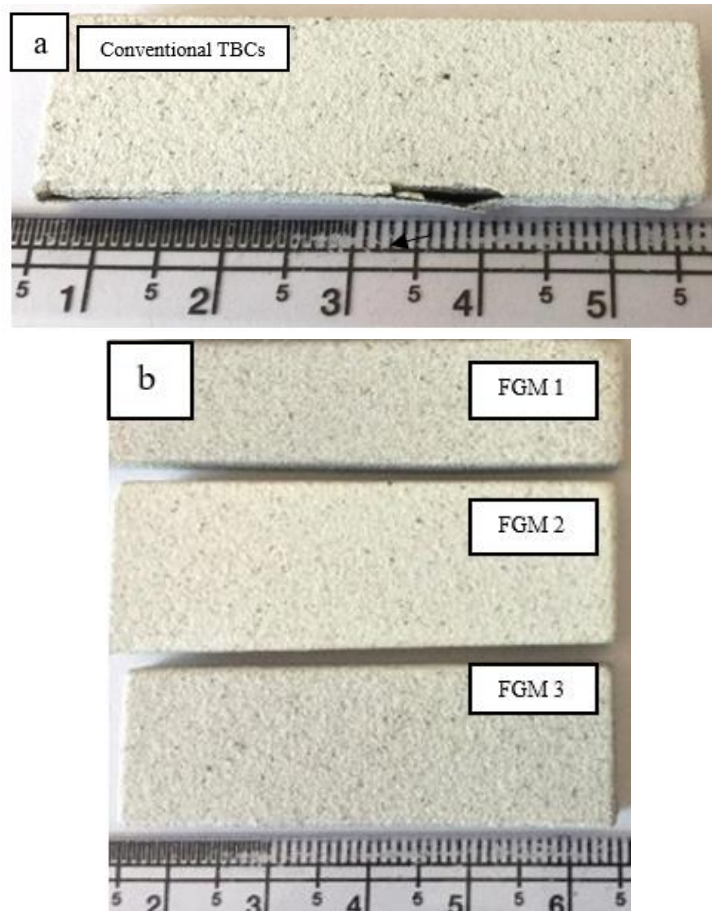


Fig 3. Oxidation stability tested specimens at 800°C:a) Conventional TBCs specimen, failed at 96 hours; b) FGM TBCs specimens after 264 hours (without cracks on the surface)

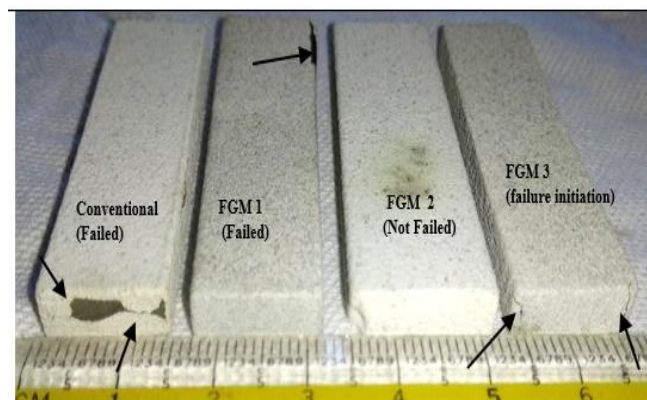


Fig 4. Oxidation stability tests at 1000°C (arrows show the failure location on the surface) [28]

Table 6. Results from oxidation stability tests (Conventional & FGM specimen) at 800 and 1000°C

S.No	Specimen Designation	No. of hours at 800°C (Cycles)/remarks	No. of hours at 1000°C (Cycles)/remarks
1	Conv TBC	96 (8)/Failed	24 (2)/ Failed
2	FGM 1	264 (22)/ Not Failed	60(5)/ Failed
3	FGM 2	264 (22)/ Not Failed	72 (6)/ Not Failed
4	FGM 3	264 (22)/ Not Failed	72 (6)/ Not Failed*

* Apparent failure due to specimen sharp edge

Table 6 shows the summarized results of oxidation stability tests at 1000°C. The improvement showed by TBCs in the functionally graded materials configurations over conventional TBCs at high temperatures is revealed.

3.5 Cross sectional metallography (SEM) after oxidation stability test

Microstructure analysis was performed on cross section metallographic specimen removed from specimen of conventional 8YSZ and FGM configurations that had undergone oxidation stability test at 800 and 1000°C. The specimen were examined under SEM with EDS facility.

Fig 5a shows a micrograph of the conventional 8YSZ specimen that has undergone oxidation stability test at 800°C for 96 hours. Characterized by severe delamination between the substrate and the bond coat, the specimen in this system failed within 96 hours of test. The top coat of the specimen in this system when subjected to oxidation stability test at 1000°C for 24 hours, which failed (shown in Fig 5) revealed largely a porous structure (Fig 5b). Microstructure of the as-sprayed coating (shown in Fig 1 a) was devoid of such porosity.

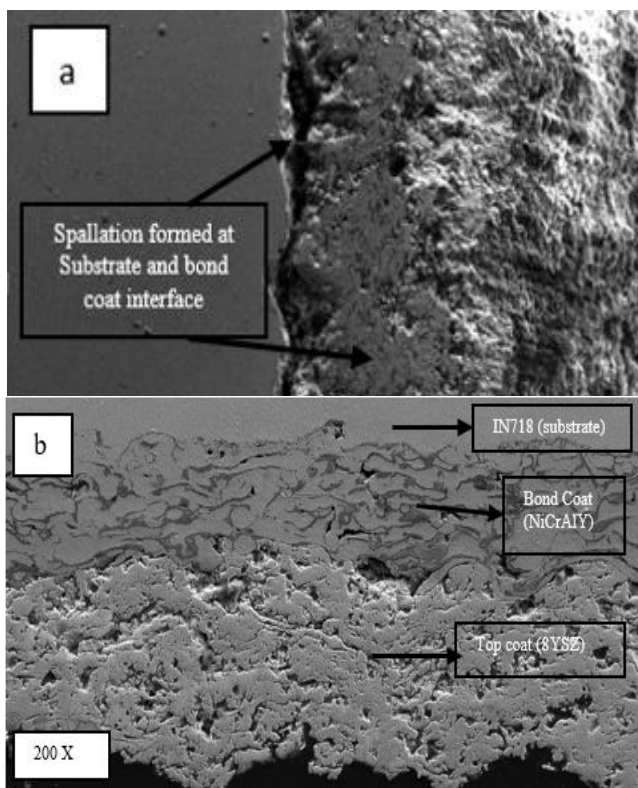


Fig 5. SEM micrograph of cross section metallographic specimen after oxidation stability test: (a) Conventional 8YSZ tested at 800°C failed at 96 hours; (b) Conventional 8YSZ tested at 1000°C failed at 24 hours

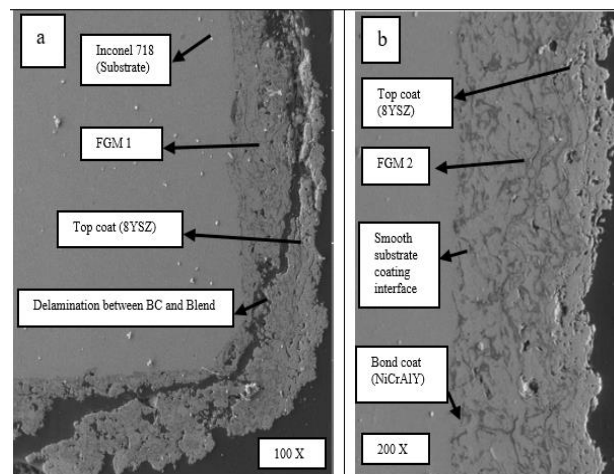


Fig 6. SEM micrographs of FGM TBCs (polished metallographic cross section) after oxidation stability test at 1000°C. a) FGM 1 b) FGM 2

SEM analysis was performed on metallographic specimen of cross section of FGM specimens (oxidation stability tested at 1000°C). SEM micrograph of FGM 1 failed in 60 hours and FGM 2 not failed after 72 hours of oxidation stability tests are shown in Fig 6 a and 6b respectively.

It is observed that detachment or delamination of layer (shown in Fig 6a (FGM1)) is formed between the blend and the ceramic top coat is due to the thermal expansion mismatch. Whereas, FGM 2 withstood 72 hours without failure signs on the surface under the same conditions is shown in Fig 6b. A certain level of surface roughness is observed due to metallography polishing of the coating.

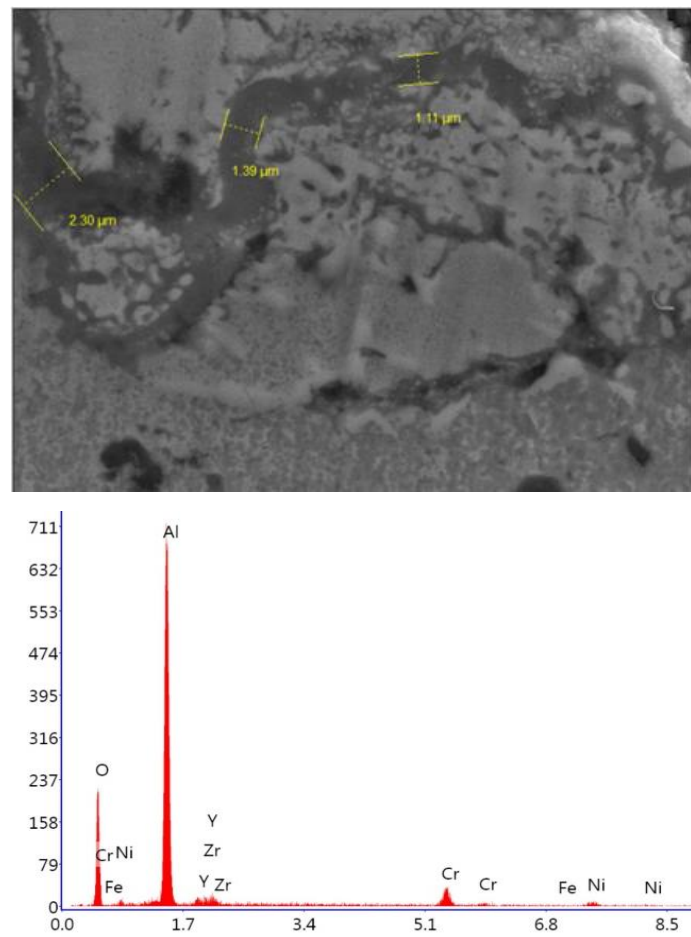


Fig 7. a) Oxide formed in between the BC and TC; **b)** EDS of conventional coating surface on selected area after oxidation test at 1000°C

Detailed examination of the cross section metallographic specimen (polished and etched) removed from Conventional TBC specimen, which was already subjected to oxidation stability test at 1000°C revealed significant oxidation within the interlayers. Fig 7a shows a typical SEM micrograph. Formation of oxide layers, ~1 to 2 μm thick, predominantly occurred between the NiCrAlY (BC) and 8YSZ (TC) layers, which pointed towards the development of thermally grown oxide TGO layers, most likely in initial stages. Confirmed via EDS analysis of on selected area of oxidation on the specimen, shown in Fig 7b, oxide scale Al_2O_3 was formed within the coated layers. This was attributable to the localized oxidation of Al resulting in the initiation of the formation of Al_2O_3 , the most likely reason for the failure of the coating.

4. Discussion

The results presented here demonstrate that the blend chemistry has a significant influence on the performance of APS TBC system. According to the established theory, the primarily driving force for TBCs failure mainly comes from the mismatch stresses induced by the difference in the coefficients of thermal expansion (CTE) between the layers. The stresses may also arise from the well-known phase transformation between the tetragonal ZrO_2 and

monoclinic ZrO_2 phase. However, the manner in which these stresses are relieved depends on the specific materials properties and thermal history (isothermal or cycled). Destabilization and extent of reformation of m- ZrO_2 , shown in table 5 does not appear to have influenced the failure, wherever it has occurred.

A significant feature observed in the microstructures (not studied in detail in this work at this stage) of as sprayed coatings of conventional and FGM TBCs is the presence of relatively large number of porosities in the conventional TBC. Blend microstructure comprised of considerably lower porosity contents. A quantitative analysis of porosity contents is beyond the scope of this paper.

The failure mechanism of thermal shock tested conventional specimens in this work may be attributed to the thermal stresses generated between the top coat (YSZ) and bond coat: in a manner similar to results reported in TBC system by C. Giolli et.al [27]. Even in oxidation stability test, the cracking and delamination of the top coat appeared to have been generated at the bond coat top coat interface, but the failure mechanism appeared to be due to the growth thermal grown oxide (TGO) layer formed at the interface that occurred by oxidation of the NiCrAlY. This effect was similar to the findings of Khor et.al [16]. In addition, large

amount of cracks also due to coalescence of existing porosity could have been formed on the ceramic top of conventional specimen which was most likely due to the sintering effect of the ceramic. Such failures (merging of porosities) evidently did not occur in FGM configuration especially where the porosities were minimum as clearly seen in FGM 2 and possibly in FGM 3 as well (not studied).

5. Conclusions

Functionally graded and a conventional thermal barrier coating of 8YSZ and NiCrAlY were synthesized using APS system. Blends of the two plasma spray powders i.e., 8YSZ and NiCrAlY in FGM configuration exhibited superior thermal shock cycle resistance over conventional TBCs. Thermal shock tests performed on the specimen at 1200°C and 1400°C demonstrated the superiority of certain blend compositions. Oxidation tests performed at 800°C to 1000°C confirmed the findings. Failures in FGM configuration, especially in 50 NiCrAlY -50 8YSZ blend composition, most likely reduced due to lowered thermal expansion coefficient mismatch. This is attributed to the gradual change in coating characteristics in FGM configuration when both, the FGM and conventional TBCs underwent tests at the same conditions. Thus the improved performance of chosen FGM configuration over conventionally synthesized TBCs and their use in terms of thermal shock resistance and oxidation resistance is unequivocally re-established.

References

- [1] N.P. Padture, M. Gell, and E.H. Jordan, Thermal barrier coatings for gas-turbine engine applications, *Science*, 296(2002) 280–284
- [2] David R. Clarke, Matthias Oechsner, and Nitin P. Padture, Thermal-barrier coatings for more efficient gas-turbine engines, *MRS Bulletin*, 37 (2012) 891- 898
- [3] X.Q. Cao, R. Vaßen and D. Stöver, Ceramic materials for thermal barrier coatings, *J. Eur. Ceram. Soc.*, 24 (2004) 1-10
- [4] Robert Vassen, Alexandra Stuke, and Detlev Stover, Recent Developments in the Field of Thermal Barrier Coatings, *Therm. Spray Technology*, 18 (2009) 181
- [5] G.A. Kawasaki and R. Watanabe, Cyclic Thermal Fracture Behavior and Spallation life of PSZ/NiCrAlY functional graded TBC, *Mater. Science Forum*, 308 (1999) 402-409
- [6] Dongming Zhu, Advanced Oxide Material Systems for 1650 °C Thermal/Environmental Barrier Coating Applications, *NASA/TM—2004-213219*, ARL-TR-3298.2004
- [7] G. Johnner and K.K. Schweitzer., Thermal Barrier Coatings for Jet Engine Improvement, *Metallurgical And Protective Coatings, Thin Solid Films*, 119 (1984) 301-315.
- [8] M. Ali, X. Chen and G. Newaz, Oxide layer development under thermal cycling and its role on damage evolution and spallation in TBC system, *J Mater Sci*, 36 (2001) 4535-4542.
- [9] Robert Vassen, Alexandra Stuke and Detlev Stover, Recent Developments in the Field of Thermal Barrier Coatings, *Thermal Spray Technology*, 18 (2009) 181.
- [10] C.U. Hardwicke Lau, Advances in Thermal Spray Coatings for Gas Turbines and Energy Generation: A Review, *J. Therm. Spray Technol.* 22(5) (2013) 564-576.
- [11] W.Y. Lee, D.P. Stinton, C.C. Berndt, F. Erdogan, Y.-D. Lee & Z. Mutasim, Concept of Functionally Graded Materials for Advanced Thermal Barrier Coating Applications, *Metallurgical and Protective Coatings, J Am Ceram Soc*, 79 (1996) 3003-3012.
- [12] Y.W. Gu, K.A. Khor, Y.Q. Fu and Y. Wang, Functionally graded ZrO₂-NiCrAlY coatings prepared by plasma spraying using pre-mixed, spheroidized powders, *Surf Coat Technol.* 96 (1997) 305-312.
- [13] Valmik Bhavar, Prakash Kattire, Sandeep Thakare, Sachin Patil and R.K.P. Singh, A Review on Functionally Gradient Materials (FGMs) and Their Applications, *IOP Conf. Series: Mater. Sci. Eng.* 229 (2017).
- [14] A. Ashofteha, M. Mosavi Mashhadi and A. Amadeh, Thermal shock behavior of multilayer and functionally graded micro- and nano-structured topcoat APS TBCs, *Ceram. Int.* 44 (2018) 1951-1963
- [15] Klod Kokini, Jeffery DeJonge, Sudarshan Rangaraj and Brad Beardsley, Thermal shock of functionally graded thermal barrier coatings with similar thermal resistance, *Surf Coat Technol.* 154 (2002) 223–231.
- [16] K.A. Khor and Y.W. Gu, Thermal properties of plasma-sprayed functionally graded thermal barrier coatings, *Thin Solid Films*, 372 (2000) 104-113.
- [17] B. Kieback, A. Neubrand and H. Riedel, Processing techniques for functionally graded materials, *Mater Sci Forum*, 362 (2003) 81-106.
- [18] M.N. Baig and F.A. Khalid, Deposition and characterization of plasma sprayed Ni-5Al/ magnesia stabilized zirconia based functionally graded thermal barrier coating, *IOP Conf. Ser.: Mater. Sci. Eng.* 60 (2014) 12053.
- [19] K.A. Khor, Z.L. Dong and Y.W. Gu, Plasma sprayed functionally graded thermal barrier coatings, *Mater. Lett.* 38 (1999) 437– 444.

- [20] Pierre Fauchais, Ghislain Montavon and Ghislaine Bertrand, From Powders to Thermally Sprayed Coatings, *J. Therm. Spray. Techn.* 19 (2010) 56–80.
- [21] Zhe Lu, Sang-Won Myoung, Yeon-Gil Jung, Govindasamy Balakrishnan, Jeongseung Lee and Ungyu Paik, Thermal Fatigue Behavior of Air-Plasma Sprayed Thermal Barrier Coating with Bond Coat Species in Cyclic Thermal Exposure, *Materials*, 6 (2013) 3387-3403.
- [22] ASTM D 6944 – 15, Standard Practice for Determining the Resistance of Cured Coatings to Thermal Cycling
- [23] W. Brand, H.J. Grabke, D. Tom and J. Kruger, The oxidation behaviour of sprayed MCrAlY coatings, *Surf. Coat. Technol.*, 87 (1996) 41-47.
- [24] G. Moskal, L. Swadźba, B. Mendala, M. Góral and M. Hetmańczyk, Degradation of the TBC system during the static oxidation test, *J. Microsc.* 237 (2009) 450-455.
- [25] Kadir Mert Doleker, Yasin Ozgurluk, Abdullah Selim Parlakyigit, Dervis Ozkan, Turgut Gulmez, Abdullah and Cahit Karaoglanli, Oxidation Behaviours of NiCr/YSZ Thermal Barrier Coatings (TBCs), *Open Chem.* 16 (2018) 876–881.
- [26] Hui Dong, Guan-Jun Yang, Cheng-Xin Li, Xiao-Tao Luo and L. Chang-Jiu, Effect of TGO Thickness on Thermal Cyclic Lifetime and Failure Mode of Plasma-Sprayed TBCs. *J. Am. Ceram. Soc.* 97(2014) 1226-1232.
- [27] C. Giolli, A. Scrivani, G. Rizzi, F. Borgioli, G. Bolelli and L. Lusvarghi, Failure Mechanism for Thermal Fatigue of Thermal Barrier Coating Systems, *J. Therm. Spray. Techn.* 18(2009) 223-230.
- [28] Kirti Teja Pasupuleti, Shawn Dsouza, Thejaraju R, Shankar Venkataraman, Parvati Ramaswamy, S.V.S. Narayana Murty, Performance and Steady State Heat Transfer Analysis of Functionally Graded Thermal Barrier Coatings Systems, *Materials Today : Proceedings (Elsevier)*, 5(2018) 27936-27945.

About The License

© 2019 The Authors. This work is licensed under a Creative Commons Attribution 4.0 International License which permits unrestricted use, provided the original author and source are credited.